Closing report of the "Characterization of the role of P53 in DNA damage induced transcriptional silencing" project

In this proposal, we aimed to study the role of ATM, DNAPK, and P53 on the ubiquitylation of the elongating form of RNAPII (S2P RNAPII) upon DSB induction. Furthermore, we aimed to monitor how P53 influences the occupancy of the stalled S2P RNAPII, reveal whether P53 affects the ubiquitylated S2P RPB1 level, and how various E3 ligases regulate this process upon different kinds of DSBs.

Project 1 The effect of ATM, DNAPK, and P53 on the ubiquitylation of S2P RNAPII

We used HCT116 p53+/+ and p53–/– isogenic colorectal carcinoma cell lines to support the potential role of P53 in transcription elongation. For this, in the abovementioned cell lines, we performed chromatin immunoprecipitation (ChIP) experiments in which we immunoprecipitated the S2P RNAPII following treatment with the transcription-blocking agent Actinomycin D (ActD). We monitored S2P RNAPII occupancy at transcriptionally active gene regions (*ACTB*, *CDK12*, and *BRAT1*) in the absence and presence of P53. As a negative control, we used primers for an intergenic region where active transcription does not occur. Our findings revealed that in HCT116 p53–/– cell line, S2P RNAPII is removed after 6 h ActD treatment, while in HCT116 p53+/+ cells, it still persists and is removed just after 24h ActD treatment, presuming that P53 delays S2P RNAPII removal from chromatin (Figure 1). Subsequently, to reveal the role of P53 and its two main activator kinases, ATM and DNAPK, in the ubiquitylation of S2P RNAPII, we performed tandem ubiquitin-binding entities (TUBE) assays in ActD-treated HCT116 p53+/+ and p53–/– cell lines using specific inhibitors against ATM and DNAPK (ATMi and DNAPKi, respectively). By this, we pulled down the polyubiquitylated protein pool, and then, with a subsequent Western blot, we monitored the changes in the level of the ubiquitylated S2P RNAPII. We observed much less ubiquitylated S2P RNAPII at 8 h ActD treatment in the absence of P53 and the loss of either ATM or DNAPK kinase activity (Figure 2). These experiments demonstrated that P53, ATM, and DNAPK play an emerging role in the polyubiquitylation-mediated removal of S2P RNAPII as a response to ActD-induced transcription blockage. However, P53 acts differently from ATM and DNAPK: P53 delays the removal of S2P RNAPII from the damaged site, while ATM and DNAPK are

indispensable for the proper activation of members of E3 ligase complexes involved in the ubiquitylation of S2P RNAPII.

To verify whether P53-mediated ubiquitylation is specific to HCT116 cell line or is a general phenomenon, we performed TUBE assays on U2OS cells. We depleted P53 with siRNA transfection, and as a control, we used non-targeting siRNA (referred to as siP53 and siSCR, respectively). Subsequently, 6 h and 24 h of ActD treatments were applied, and the ubiquitylated protein pool was captured by TUBEs pull-down; then, changes in the level of ub-S2P RNAPII were detected by Western blot. In siSCR-transfected U2OS cells, following 6 h ActD treatment, a relatively high amount of ub-S2P RNAPII was observed, which was decreased 24 h after ActD treatment. Similar kinetics, but less ub-S2P RNAPII was detected in siP53-transfected samples. Furthermore, following 24 h ActD treatment, the total protein level of S2P RNAPII remained accumulated in siP53-transfected cells, while it was diminished by that time point in mock siRNA-transfected cells. The efficiency of P53 silencing was verified by Western blot using a P53-specific antibody (Figure 3). These results support our previous TUBEs assay performed on HCT116 p53+/+ and p53-/- cells, advocating a ubiquitous role of p53 in the ubiquitylation of S2P RNAPII as a response to transcription block.

Since in the ChIP experiment, we found a much faster dislodgement of S2P RNAPII from the damaged chromatin, and in TUBE, less ubiquitylated S2P RNAPII was detected in the absence of P53, we hypothesized that S2P RNAPII had been already ubiquitylated and degraded by 8 h ActD. To confirm our assumption, we performed an additional TUBE assay, where we monitored the alterations in the level of the ubiquitylated S2P RNAPII following 1 h, 4 h and 8 h ActD treatments. We showed that following 1 h ActD treatment, more polyubiquitylated S2P RNAPII were precipitated in the absence of P53, while in the presence of P53, we detected a high amount of ubiquitylated S2P RNAPII only at 8 h ActD (Figure 4). From this, we demonstrated that P53 plays a negative role in the premature ubiquitylation of S2P RNAPII. Therefore, we unveiled that P53 delays the turnover of S2P RNAPII from the damaged chromatin to protect it from preliminary degradation and ensure time for proper DNA repair.

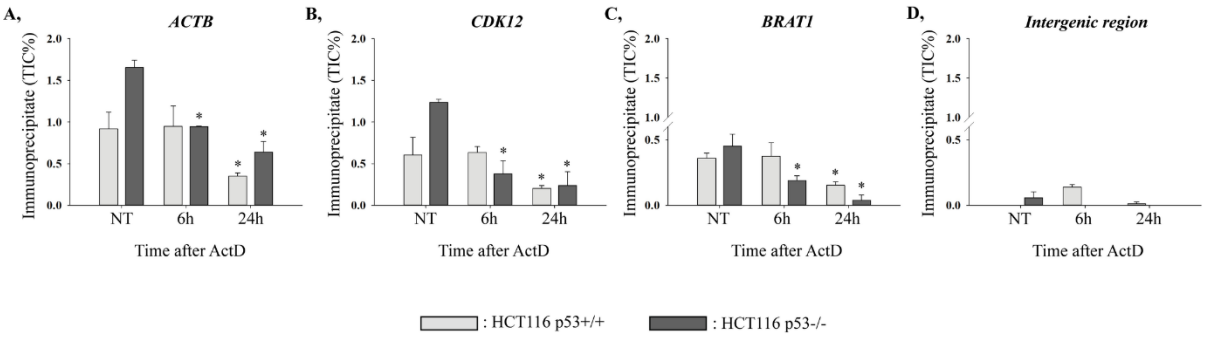

Figure 1 P53 affects the profile changes of elongating RNA polymerase II (S2P RNAPII) at transcriptionally active gene regions following Actinomycin D (ActD)-induced transcription elongation block. (**A–C**) S2P RNAPII occupancy was monitored with ChIP–qPCR at *ACTB*, *CDK12*, and *BRAT1* gene bodies in the presence (light grey columns; HCT116 p53+/+ cell line) and in the absence (dark grey columns; HCT116 p53-/- cell line) of P53. The profile changes were tracked under physiological conditions (NT) as well as following 6 h and 24 h ActD treatments. (**D**) Primers designed for an intergenic region were used as the negative control of the ChIP. The figure shows the representative result of one out of two independent experimental replicates. qPCR reactions were performed in duplicates. Asterisks represent statistical significance (*P ≤ 0.05) between the mean values. The mean values of ActD-treated samples were compared to the mean value of the corresponding non-treated sample by one-way ANOVA in the case of each cell line.

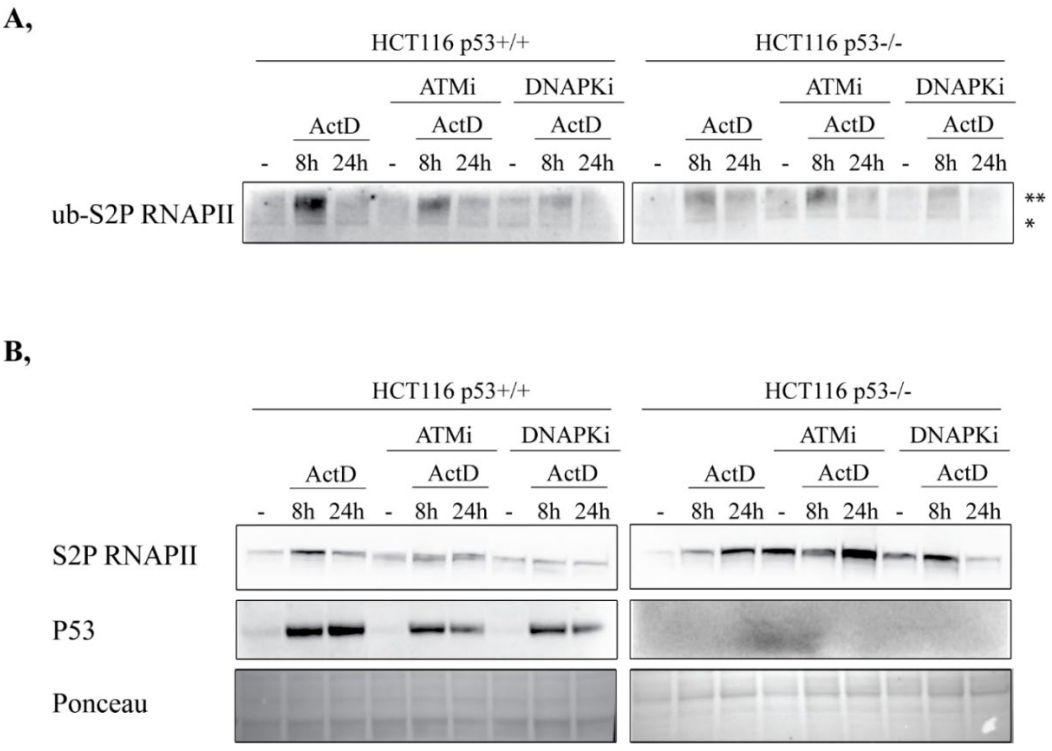

Figure 2 P53, Ataxia-telangiectasia mutated (ATM), and DNA-dependent protein kinase (DNAPK) influence the ubiquitylation of S2P RNAPII as a response to ActD treatment. (**A**) Tandem ubiquitin-binding entities (TUBEs) pull-down, followed by Western blot detection, was performed in HCT116 p53+/+ (left panel) and p53-/- (right panel) cells. TUBEs experiment was accomplished under physiological conditions as well as 8 h and 24 h following ActD treatment in the presence or the absence of ATMi or DNAPKi. From the pulled-down ubiquitylated protein pool, polyubiquitylated S2P RNAPII (ub-S2P RNAPII) was detected with anti-S2P RNAPII

antibody. *: monoubiquitylated S2P RNAPII, **: polyubiquitylated S2P RNAPII (**B**) Western blot experiment on whole cell lysates of HCT116 p53+/+ (left panel) and p53-/- (right panel), which were used for TUBEs pull-down assay. Total protein level changes of S2P RNAPII and P53 following 8 h and 24 h ActD treatment in the presence or the absence of ATMi or DNAPKi were immunodetected using specific antibodies. Ponceau staining was applied to detect the equal loading of the input samples.

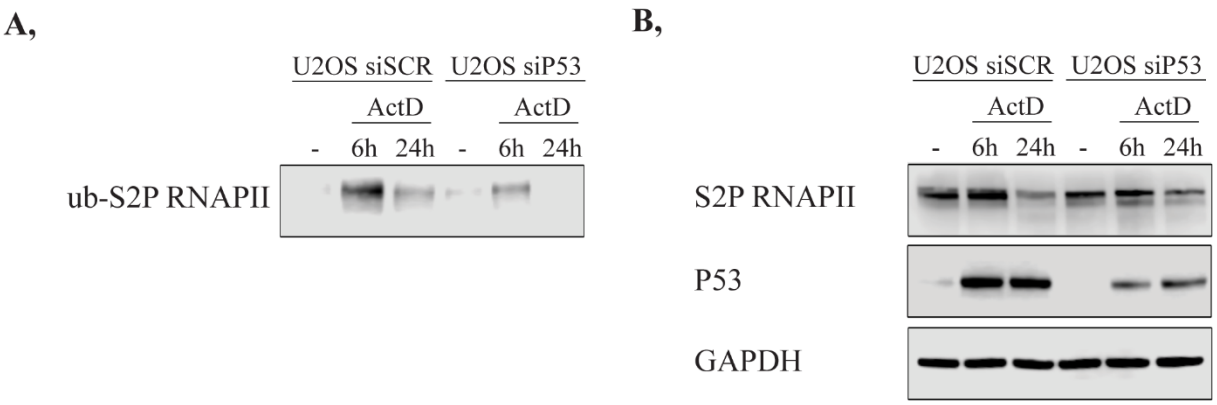

Figure 3 P53 involvement in the ubiquitylation of RNAPII following ActD treatment is a ubiquitous process. (**A**) Tandem ubiquitin-binding entities (TUBEs) pull-down, followed by Western blot detection, was performed in non-targeting- and P53 silencing siRNA- transfected (referred to as siSCR and siP53) U2OS cells. In U2OS cells, TUBEs assay was performed under physiological conditions, 6 h and 24 h following ActD treatment. From the pulled-down ubiquitylated protein pool, polyubiquitylated S2P RNAPII (ub-S2P RNAPII) was detected with anti-S2P RNAPII antibody. (**B**) Western blot experiment on whole cell lysates of U2OS cells, which were used for TUBEs pull-down assay. Total protein level changes of S2P RNAPII and P53 were followed as a response to 6 h and 24 h ActD treatment and were immunodetected using specific antibodies. GAPDH detection was applied to detect the equal loading of the input samples.

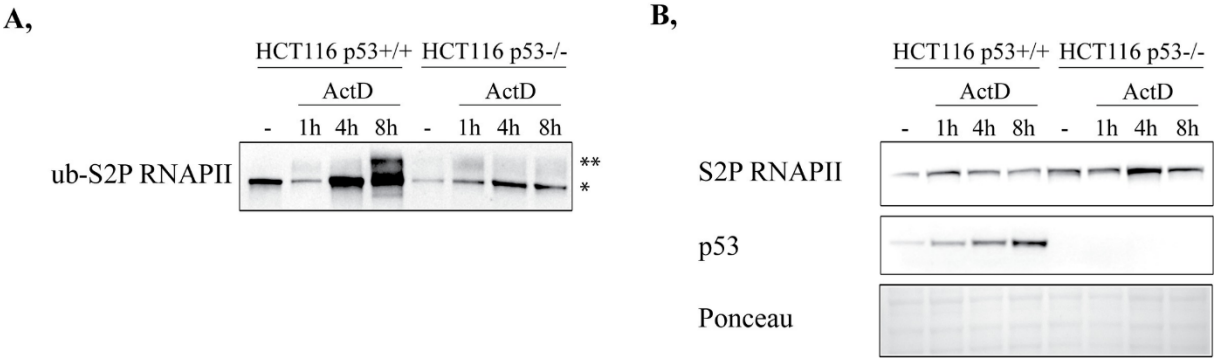

Figure 4 P53 is essential for preventing the premature ubiquitylation of RNAPII following ActD treatment. (**A**) Tandem ubiquitin-binding entities (TUBEs) pull-down, followed by Western blot detection, was performed in HCT116 p53+/+ and p53-/- cells. TUBEs experiment was accomplished under basal conditions as well as 1 h, 4 h, and 8 h following ActD. From the pulled-down ubiquitylated protein pool, polyubiquitylated S2P RNAPII (ub-S2P RNAPII) was detected with anti-S2P RNAPII antibody. *: monoubiquitylated S2P RNAPII, **: polyubiquitylated S2P RNAPII. (**B**) Western blot experiment on whole cell lysates of HCT116 p53+/+ and p53-/-, which were used for TUBEs pull-down assay. Total protein level changes of S2P RNAPII and P53 following 1

h, 4 h, and 8 h ActD treatments in HCT116 cells were immunodetected using specific antibodies. Ponceau staining was applied to detect the equal loading of the input samples.

The above-described results were published in the *Plos One* journal in 2022 as a first-author article of mine [1]. Furthermore, in 2020, two additional first-author reviews were also successfully published related to the DSB- and NER-related ubiquitylation cellular processes in *Cancers* and *Cells*, respectively [2,3]. Two co-author methodology-based review articles corresponding to the generation and visualization of DSBs and the visualization and quantification of endonuclease-based site-specific DNA damage were reported in *Mutation Research–Reviews in Mutation Research* and *JoVE* in 2021 [4,5]. In accordance with the transcription-coupled stress response, we established a collaboration with John Rouse, and we revealed that CDKL5 kinase activity is indispensable for the proper transcriptional inhibition following DSBS. From this project, a co-authored article was reported in *EMBO Journal* in 2021 [6].

Project 2 Identifying factors involved in the degradation of RNAPII upon DNA double-strand breaks

To identify E3 ligases that participate in the ubiquitylation of the transcriptionally engaged RNAPII, we immunoprecipitated the elongating form of RNAPII (denoted to S2P RNAPII) and performed LC-MS/MS analyses. From the list of possible targets, we identified the E3 ligases WWP2 and NEDD4, and the CUL3 scaffold protein of the CRL3 ligase complexes as the most significant hits that can be relevant for further investigation. To verify these results, we performed reciprocal immunoprecipitations by pulling down WWP2, NEDD4 and S2P RNAPII, and the total RNAPII. In the case of CUL3, due to the lack of efficient commercial antibodies, we could only immunoprecipitate it and prove the interaction using overexpression with the plasmid pCDNA3.1-MYC-CUL3.

Our next aim was to reveal whether these ligases play a direct role in DSB-mediated transcription regulation. To explore this, we first established an inducible U2OS-derived cell line stably expressing the restriction endonuclease AsiSI (referred to as VAsiSI). With Doxycycline (DOX) treatment, the cytoplasmic sequestration of AsiSI can be induced, and additional 4-hydroxitamoxifen (4-OHT) treatment facilitates its nuclear translocation where it can recognize and cut its target restriction sites (Figure 5A–B). We monitored the cutting efficiency of 10 genes, from which we selected 2 to examine the effect of the E3 ligase knockdown. Using siRNAs, we knocked down WWP2, NEDD4, and CUL3 in VAsiSI cells

and induced directed DSBs with 4-OHT treatment. Upon DSB induction with 4-OHT, the mRNA levels of those genes were efficiently reduced when non-targeting siRNAs (denoted to siSCR) were used. We found that WWP2, NEDD4, and CUL3 knockdown rescued transcription despite DSBs (Figure 5C). These findings are further supported in a previously established stable cell line in which I-PpoI restriction endonuclease can be inducibly expressed (referred to as U2OS-pEP15, Figure 5D).

In addition, to verify these results at the global genomic level, we used the radiomimetic drug neocarzinostatin (NCS) in U2OS cells to induce random global DSBs. We took advantage of the Click-iT chemistry to fluorescently label *de novo* synthesized RNA transcripts following the knockdown of each E3 ligase. In siSCR cells, the number of fluorescent foci was remarkably reduced after 4 h NCS treatment, whereas ligase silencing resulted in increased foci count, indicating an upregulation of gene expression instead of a total transcription shut-down (Figure 5E). By this, we could establish proof of a direct connection between the ligases mentioned above and DSB-mediated transcription regulation.

Subsequently, we wanted to unravel the mechanisms lying behind this phenomenon. For this, we performed Western blot experiments to track the changes in the level of S2P RNAPII upon NCS treatment of the cell lines in which each ligase was solely depleted. We detected accumulated S2P RNAPII levels upon abrogation of each of the desired ligases, suggesting a deterioration in the ubiquitylation of S2P RNAPII. Nevertheless, this is not a direct link with the ubiquitylation-assisted damage resolution, and for this, we continued our investigation by using tandem ubiquitin-binding entities (TUBEs) to pull down all the ubiquitylated proteins after ligase silencing and robust damage induction. Our findings unveil that WWP2 profoundly impacts the ubiquitylation of S2P RNAPII both under physiological conditions and upon DSB induction. On the other hand, NEDD4 had relevant connections only upon DSB induction, whereas CUL3 had a mild effect under these conditions.

To decipher the ubiquitylation code of S2P RNAPII, we took advantage of the Ubiquitin Chain Restriction Analysis protocol (UbiCREST) which utilizes the linkage specificity of the Ovarian Tumor Domain (OTU) class of Deubiquitinases (DUBs) to characterize the linkages present in a sample containing polyubiquitin. S2P RNAPII was immunoprecipitated and treated with USP2/USP21 (pan-DUBs), OTUB1 (cleaves K48-linkage chains), and AMSH (cleaves K63-linkage types) while the result was visualized with Western blot using an antibody which is specific to ubiquitin. The reciprocal experiment was also performed using TUBE beads and blotting against S2P RNAPII. For these experiments, we used NCS and 4 Gy Ionizing radiation.

We could establish for the first time that upon DSBs, S2P RNAPII is ubiquitylated primarily at K63 chains and that K48-linkages mainly participate in normal protein turnover.

To further explore the involvement of each ligase in this process, we overexpressed the plasmids pCDNA3.1-HA-Ub-wt (overexpression of all linkage types), pCDNA3.1-HA-Ub-K0 (no overexpression of any known linkage type), pCDNA3.1-HA-Ub-K63 (overexpression of only K63 linkage types), and pCDNA3.1-HA-Ub-K48 (overexpression of only K48 linkage types) and immunoprecipitated S2P RNAPII in the presence or absence of DSBs. We revealed that WWP2 knockdown reduced both K63 and K48 linkage types in both NT and DSB conditions, whereas NEDD4 knockdown remarkably reduced both linkage types only in the case of DSB induction. On the other hand, silencing CUL3 reduced K48-linked ubiquitin chains only under physiological conditions.

Moreover, in the knockdown cell lines, we performed subcellular fractionation to monitor the level of chromatin-bound S2P RNAPII following DSB induction. We demonstrate that NEDD4 and CUL3 knockdown remarkably increased the chromatin-bound fraction of S2P RNAPII in response to DSBs. However, WWP2 knockdown resulted in the accumulation of the chromatin-bound S2P RNAPII with no changes across the conditions (Figure 6).

All in all, our results unravel an intricate mechanism governed by the aforementioned E3 ubiquitin ligases, regulating fine-tuned transcription silencing following DSB induction. Our project would establish a solid foundation for targeted cancer therapies by exploiting our novel findings and insights into E3 ligases that could potentially be used in the PROTAC technology.

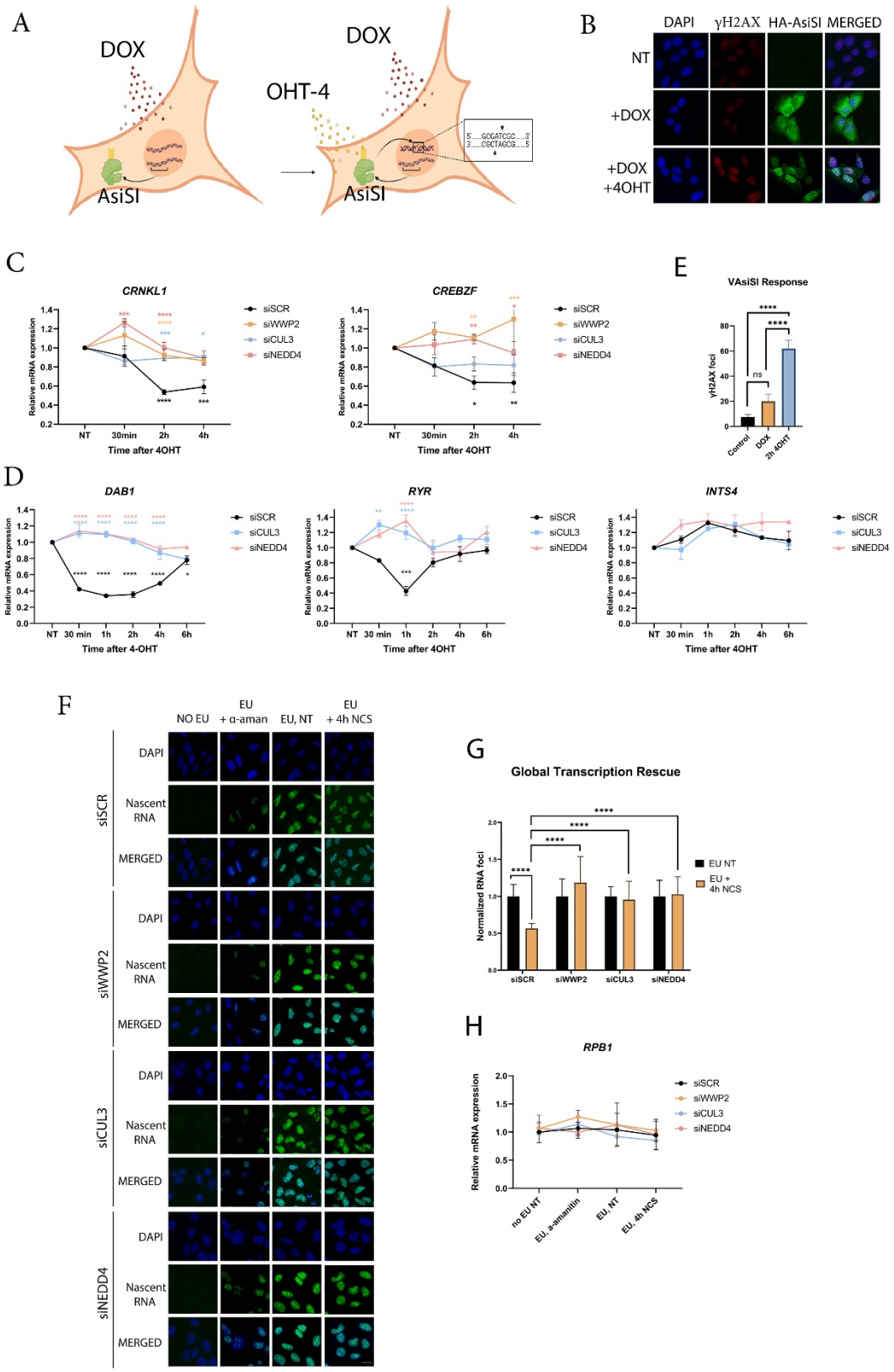

Figure 5 WWP2, CUL3, and NEDD4 play a promiscuous role in DSB-induced transcriptional silencing. A) The schematic representation of the inducible VAsiSI cell line. Upon doxycycline (DOX) addition, the cytoplasmic expression of AsiSI is initiated, then 4-OHT administration induces the nuclear translocation of AsiSI restriction

endonuclease which can cut DNA site-specifically. B) Immunofluorescence staining of DOX and DOX+4-OHT-induced VASiSI cells with HA and yH2AX antibodies. HA antibody makes monitoring the subcellular localization of the HA-ER-ASiSI fusion protein possible, while the yH2AX antibody makes visible those DSB foci at which AsiSI have cut. C) Monitoring the effect of WWP2, NEDD4, and CUL3 on transcription silencing in the VAsiSI cell line. As a negative control, siSCR was used. D) Monitoring the effect of NEDD4 and CUL3 on transcription silencing in I-PpoI restriction endonuclease-expressing cell lines. E) Quantification of the induced yH2AX foci number in VAsiSI cell line. F) Click-iT chemistry to fluorescently label *de novo* synthesized RNA transcripts in siSCR, siWWP2, siNEDD4, and siCUL3 transfected U2OS cells. G) Quantification of the Click-iT results. H) Relative mRNA expression of RPB1 following those conditions which were used in the Click-iT chemistry.

Figure 6 NEDD4 and CUL3 knockdown remarkably increased the chromatin-bound fraction of S2P RNAPII in response to DSBs, while WWP2 knockdown resulted in the accumulation of the chromatin-bound S2P RNAPII with no changes across the conditions. Nuclear soluble and insoluble fraction isolation from non-treated and neocarzinostatin (NCS)-treated (0.5, 2, 4, and 8 h) U2OS cells following silencing WWP2 (siWWP2), CUL3 (siCUL3), or NEDD4 (siNEDD4). As a negative control, non-targeting siRNA (siSCR) was used. The changes in the level of S2P RNAPII were monitored using an S2P RNAPII antibody. Lamin A/C and yH2AX antibodies were used to verify the success of the fractionation. The latter was also used to validate the efficiency of NCS treatment.

Regarding the importance of the cytoplasmic aggregation of RPB1 in patients with invasive breast cancer, we published a co-authored article in *IJMS* in 2023 [7].

Besides the above-listed articles, several additional projects, which are not directly related to the OTKA proposal but correspond to DNA repair, were involved in my grant. In 2022, I published a first- and last-authored article (*Cells*) about breast cancer-related microRNAs, in which we found that miR-15a+miR-16+miR-221 multiple miRNAs would be a suitable target in diagnosing BC even in the early stage [8]. In 2023, a review article related to breast cancer diagnostics was published by the correspondence of Tibor Pankotai in *Journal of Biotechnology* [9]. As a co-author, I was involved in writing a review about PARylation during transcription, published in *Cancers* in 2020 [10]. I also participated in a project demonstrating that SPB10 protein is implicated in UV-induced stress as a “quality control protein,” presumably by slowing

down the repair process—it was published in *IJMS* in 2021 [11]. In 2022, we successfully published an article about the clinical significance of epigenetic markers and RNAPII in clear cell renal carcinoma (*Translational Oncology*) [12], and another article about the potential role of certain Drosophila deubiquitylases (*Scientific Reports*) [13]. In 2022, a last-authored article of Tibor Pankotai about the transcription-related characterization of clear cell renal carcinoma was reported in *Pathology and Oncology Research* [14]. Finally, in 2023, a co-authored article of mine about the importance of finding the most suitable reference gene in a particular experimental setup was reported in *Biomolecules* [15].

In conclusion, we published 15 articles, including 2 D1 and 8 Q1. The participants of OTKA-FK 132080 actively participated in several international conferences where the above-described findings were presented in the form of posters and presentations as well.

1. Borsos, B.N.; Pantazi, V.; Páhi, Z.G.; Majoros, H.; Ujfaludi, Z.; Berzsenyi, I.; Pankotai, T. The role of p53 in the DNA damage-related ubiquitylation of S2P RNAPII. *Plos One* **2022**, *17*, doi:ARTN e0267615 10.1371/journal.pone.0267615.
2. Borsos, B.N.; Majoros, H.; Pankotai, T. Ubiquitylation-Mediated Fine-Tuning of DNA Double-Strand Break Repair. *Cancers* **2020**, *12*, doi:ARTN 1617 10.3390/cancers12061617.
3. Borsos, B.N.; Majoros, H.; Pankotai, T. Emerging Roles of Post-Translational Modifications in Nucleotide Excision Repair. *Cells-Basel* **2020**, *9*, doi:ARTN 1466 10.3390/cells9061466.
4. Berzsenyi, I.; Pantazi, V.; Borsos, B.N.; Pankotai, T. Systematic overview on the most widespread techniques for inducing and visualizing the DNA double-strand breaks. *Mutat Res-Rev Mutat* **2021**, *788*, doi:ARTN 108397 10.1016/j.mrrev.2021.108397.
5. Pantazi, V.; Berzsenyi, I.; Borsos, B.N.; Pankotai, T. Visualizing and Quantifying Endonuclease-Based Site-Specific DNA Damage. *Jove-J Vis Exp* **2021**, ARTN e62175 10.3791/62175, doi:ARTN e62175 10.3791/62175.
6. Khanam, T.; Munoz, I.; Weiland, F.; Carroll, T.; Morgan, M.; Borsos, B.N.; Pantazi, V.; Slean, M.; Novak, M.; Toth, R., et al. CDKL5 kinase controls transcription-coupled responses to DNA damage. *Embo J* **2021**, *40*, e108271, doi:10.15252/embj.2021108271.
7. Nagy-Mikó, B.; Németh-Szatmári, O.; Faragó-Mészáros, R.; Csókási, A.; Bognár, B.; Ördög, N.; Borsos, B.N.; Majoros, H.; Ujfaludi, Z.; Oláh-Németh, O., et al. Predictive Potential of RNA Polymerase B (II) Subunit 1 (RPB1) Cytoplasmic Aggregation for Neoadjuvant Chemotherapy Failure. *International Journal of Molecular Sciences* **2023**, *24*, doi:ARTN 15869 10.3390/ijms242115869.
8. Borsos, B.N.; Páhi, Z.G.; Ujfaludi, Z.; Sükösd, F.; Nikolényi, A.; Bankó, S.; Pankotai-Bodó, G.; Oláh-Németh, O.; Pankotai, T. BC-miR: Monitoring Breast Cancer-Related miRNA Profile in Blood Sera-A Prosperous Approach for Tumor Detection. *Cells-Basel* **2022**, *11*, doi:ARTN 2721 10.3390/cells11172721.
9. Pankotai-Bodo, G.; Olah-Nemeth, O.; Sukosd, F.; Pankotai, T. Routine molecular applications and recent advances in breast cancer diagnostics. *J Biotechnol* **2024**, *380*, 20-28, doi:10.1016/j.jbiotec.2023.12.005.
10. Páhi, Z.G.; Borsos, B.N.; Pantazi, V.; Ujfaludi, Z.; Pankotai, T. PARylation During Transcription: Insights into the Fine-Tuning Mechanism and Regulation. *Cancers* **2020**, *12*, doi:ARTN 183 10.3390/cancers12010183.

11. Majoros, H.; Borsos, B.N.; Ujfaludi, Z.; Páhi, Z.G.; Mórocz, M.; Haracska, L.; Boros, I.M.; Pankotai, T. SerpinB10, a Serine Protease Inhibitor, Is Implicated in UV-Induced Cellular Response. *International Journal of Molecular Sciences* **2021**, *22*, doi:ARTN 8500
10.3390/ijms22168500.
12. Ördög, N.; Borsos, B.N.; Majoros, H.; Ujfaludi, Z.; Pankotai-Bodó, G.; Bankó, S.; Sükösd, F.; Kuthi, L.; Pankotai, T. The clinical significance of epigenetic and RNAPII variabilities occurring in clear cell renal cell carcinoma as a potential prognostic marker. *Transl Oncol* **2022**, *20*, doi:ARTN 101420
10.1016/j.tranon.2022.101420.
13. Páhi, Z.G.; Kovács, L.; Szucs, D.; Borsos, B.N.; Deák, P.; Pankotai, T. Usp5, Usp34, and Otu1 deubiquitylases mediate DNA repair in. *Sci Rep-Uk* **2022**, *12*, doi:ARTN 5870
10.1038/s41598-022-09703-x.
14. Ujfaludi, Z.; Kuthi, L.; Pankotai-Bodó, G.; Bankó, S.; Sükösd, F.; Pankotai, T. Novel Diagnostic Value of Driver Gene Transcription Signatures to Characterise Clear Cell Renal Cell Carcinoma, ccRCC. *Pathol Oncol Res* **2022**, *28*, doi:ARTN 1610345
10.3389/pore.2022.1610345.
15. Barta, N.; Ördög, N.; Pantazi, V.; Berzsenyi, I.; Borsos, B.N.; Majoros, H.; Páhi, Z.G.; Ujfaludi, Z.; Pankotai, T. Identifying Suitable Reference Gene Candidates for Quantification of DNA Damage-Induced Cellular Responses in Human U2OS Cell Culture System. *Biomolecules* **2023**, *13*, doi:ARTN 1523
10.3390/biom13101523.